$\Delta I = \frac{1}{2}$ weak baryon decays

R. E. Karlsen, W. H. Ryan, and M. D. Scadron
Physics Department, University of Arizona, Tucson, Arizona 85721
(Received 14 May 1990)

First we extract phenomenological values for the reduced matrix elements $\langle B'|H_w^{PC}|B \rangle$ and $\langle B|H_w^{PV}|D \rangle$ connected with octet-baryon $B \to B'\pi, B'\gamma$ weak decays and decuplet decays $D \to B\pi$. Then we show at the quark level that the combination of $\Delta I = \frac{1}{2}$ quark W-exchange and self-energy graphs explains $\langle B'|H_w^{PC}|B \rangle$ transitions better than either separately. However, only the self-energy graph can contribute to $\langle \Xi|H_w^{PV}|\Omega \rangle$. This overall picture gives an excellent fit to over ten nonleptonic weak baryon decays.

I. INTRODUCTION

There is much data for $\Delta S = 1$ nonleptonic weak baryon decays $B \to B'\pi$ (14 amplitudes), $B \to B'\gamma$ (4 amplitudes), $D \to B\pi$ (3 amplitudes), where B, B' are octet baryons and D are decuplet baryons. All of these weak transitions empirically are dominated by a weak Hamiltonian density H_w transforming as $\Delta I = \frac{1}{2}$. Although the current-algebra–partially-conserved-axial-vector-current (PCAC) program gives an approximate hadron picture,[1] a detailed quark interpretation of the $\Delta I = \frac{1}{2}$ rule for all 21 of the above $B \to B'\pi, B'\gamma$ and $D \to B\pi$ weak transitions has yet to be understood.

In this paper we propose such a $\Delta I = \frac{1}{2}$ quark picture based on the standard weak first-order perturbation theory for $\langle \pi B'|H_w|B, D \rangle$. First, in Sec. II, we study p-wave $B \to B'\pi$ decays and apply the pole model to convert the measured[2] $\langle \pi B'|H_w^{PC}|B \rangle$ parity-conserving (PC) weak transitions to reduced $\langle B'|H_w^{PC}|B \rangle$ matrix elements. The latter are then reconfirmed in Sec. III from observed $B \to B'\gamma$ decays. In Sec. IV, we attempt to explain these reduced PC matrix elements in terms of the $\Delta I = \frac{1}{2}$ W-exchange[3–5] quark-model Hamiltonian H_{Wx}, but find that this model can only recover about one-half of the $\langle p|H_w^{PC}|\Sigma^+ \rangle$, $\langle n|H_w^{PC}|\Sigma^0 \rangle$, $\langle n|H_w^{PC}|\Lambda \rangle$, and $\langle \Lambda|H_w^{PC}|\Xi^0 \rangle$ transitions, while completely failing to predict the nonvanishing $\langle \Sigma|H_w^{PC}|\Xi \rangle$ reduced matrix elements. Next in Sec. V we review $D \to B\pi$ weak decays, applying current algebra and PCAC to extract the parity-violating (PV) transitions $\langle B|H_w^{PV}|D \rangle$ and demonstrating that the latter empirical $\langle \Xi|H_w^{PV}|\Omega \rangle$ transition is dominated by a kaon PV tadpole. Then in Sec. VI we suggest that this $\Delta I = \frac{1}{2}$ PV reduced matrix element has a quark (tadpole) interpretation as an s-d self-energy transition Σ_{sd}^{PV}, which cannot be "transformed away." In Sec. VII, we extend this quark self-energy Hamiltonian to Σ_{sd}^{PC} and show that the empirical octet-baryon PC transitions $\langle p|H_w^{PC}|\Sigma^+ \rangle$, $\langle n|H_w^{PC}|\Lambda \rangle$, and $\langle \Lambda|H_w^{PC}|\Xi^0 \rangle$ can acquire about one-half their values from this Σ_{sd}^{PC} Hamiltonian. Finally, in Sec. VIII, we summarize our results and show that the combined $\Delta I = \frac{1}{2}$, $\Delta S = 1$ quark Hamiltonian

$H_{Wx} + \Sigma_{sd}$ can explain all measured $B \to B'\pi$, $B \to B'\gamma$, $D \to B\pi$ nonleptonic weak decays.

II. OCTET-BARYON $B \to B'\pi$ DECAYS

First we separate $B \to B'\pi$ weak transition amplitudes into their s-wave parity-violating (PV) and p-wave parity-conserving (PC) parts: $M = -\langle B'\pi|H_w|B \rangle = \bar{u}_{B'}(iA + B\gamma_5)u_B$, with spinors normalized covariantly $\bar{u}u = 2m_B$. The decay rates and asymmetry parameters are then used to determine the (real) amplitudes A and B (neglecting final-state interactions):

$$\Gamma(B \to B'_\pi) = (p/8\pi m_B^2)(a^2 + b^2) , \tag{1a}$$

$$\alpha(B \to B'_\pi) = \frac{2ab}{a^2 + b^2} , \tag{1b}$$

where $a = [(m_B + m_{B'})^2 - m_\pi^2]^{1/2}A$ and $b = [(m_B - m_{B'})^2 - m_\pi^2]^{1/2}B$. Taking the most recent Particle Data Group Compilation,[2] Eqs. (1) then lead to the seven PV and seven PC amplitudes tabulated[6] in Table I. Since the PV pole terms are suppressed by the SU(3) null theorem $\langle B'|H_w^{PV}|B \rangle \approx 0$, here we focus instead on the dominant PC pole terms as in Ref. 7. To extract the most model-independent results, we shall avoid SU(3) assumptions for $\langle B'|H_w^{PC}|B \rangle$, using instead only the SU(2) $\Delta I = \frac{1}{2}$ relations. However, we will assume the strong vertex in p-wave pole terms obeys the usual SU(3) pattern

$$H_{B'PB} = 2g\bar{B}^f(d_P d_{fji} + if_P f_{fji})P^j\gamma_5 B^i$$

$$= g_{\pi B'B}\bar{B}'\gamma_5 BP , \tag{2}$$

where $g = g_{\pi NN} \approx 13.4$ and $(d/f)_A \approx 1.74$ is the semileptonic d/f ratio,[8] equivalent to $(d/f)_P$ via PCAC. These strong couplings are tabulated in Table II for Cartesian phases of baryon states in (2) as used in Table I.

The simplest p-wave decay for $\Sigma^+ \to p\pi^0$ is depicted by the pole graphs in Fig. 1. Its PC amplitude B listed in Table I is

TABLE I. Observed hyperon decay amplitudes.

		s wave $10^6 A$	p wave $10^6 B$
(Λ_-^0)	$\Lambda \rightarrow p\pi^-$	0.323 ± 0.002	2.20 ± 0.05
(Λ_0^0)	$\Lambda \rightarrow n\pi^0$	-0.237 ± 0.003	-1.59 ± 0.14
(Σ_0^+)	$\Sigma^+ \rightarrow p\pi^0$	-0.326 ± 0.011	2.67 ± 0.15
(Σ_+^+)	$\Sigma^+ \rightarrow n\pi^+$	0.014 ± 0.003	4.22 ± 0.01
(Σ_-^-)	$\Sigma^- \rightarrow n\pi^-$	0.427 ± 0.002	-0.14 ± 0.02
(Ξ^-)	$\Xi^- \rightarrow \Lambda\pi^-$	-0.450 ± 0.002	1.75 ± 0.06
(Ξ_0^0)	$\Xi^0 \rightarrow \Lambda\pi^0$	0.344 ± 0.006	-1.22 ± 0.07

FIG. 1. Octet-pole graphs for $\Sigma^+ \rightarrow p\pi^0$ decay.

$$B(\Sigma_0^+) = -\frac{\langle p|H_w^{PC}|\Sigma^+\rangle}{m_\Sigma - m_p}(g_{\pi^0 pp} - g_{\pi^0 \Sigma^+ \Sigma^+})$$
$$= (2.67 \pm 0.15) \times 10^{-6} . \qquad (3)$$

where Σ_0^+ refers to $\Sigma^+ \rightarrow p\pi^0$. Then (3) requires, from (2) and Table II,

$$\langle p|H_w^{PC}|\Sigma^+\rangle = -180 \pm 10 \text{ eV} . \qquad (4)$$

Given (4) we study $\Lambda \rightarrow p\pi^-$ with associated p-wave pole amplitude

$$B(\Lambda_-^0) = \frac{g_{\pi^-\Sigma^+\Lambda}\langle p|H_w^{PC}|\Sigma^+\rangle}{m_\Sigma - m_p} - \frac{g_{\pi^- pn}\langle n|H_w^{PC}|\Lambda\rangle}{m_\Lambda - m_n} . \qquad (5)$$

Since we know $\langle p|H_w^{PC}|\Sigma^+\rangle$ from Eq. (4) and $B(\Lambda_-^0)$ from Table I we can find a value for $\langle n|H_w^{PC}|\Lambda\rangle$ from (5):
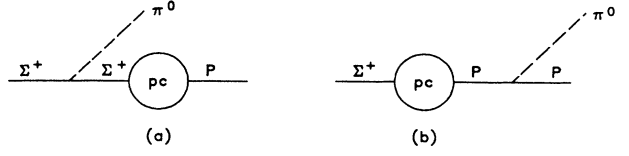
$$\langle n|H_w^{PC}|\Lambda\rangle = -87 \pm 4 \text{ eV} . \qquad (6)$$

Now self-consistency comes into play. We have *three* decays remaining $(\Lambda_0^0, \Sigma_-^-, \Sigma_+^+)$ in which to determine *one* amplitude $\langle n|H_w^{PC}|\Sigma^0\rangle$. If our approach is valid, the three decays must give the same numerical answer for $\langle n|H_w^{PC}|\Sigma^0\rangle$. By examining the pole graphs for Λ_0^0, Σ_+^+, and Σ_-^- transitions one finds the PC amplitudes

$$B(\Lambda_0^0) = \frac{g_{\pi^0 \Sigma^0 \Lambda}\langle n|H_w^{PC}|\Sigma^0\rangle}{m_\Sigma - m_n} - \frac{g_{\pi^0 nn}\langle n|H_w^{PC}|\Lambda\rangle}{m_\Lambda - m_n} , \qquad (7a)$$

TABLE II. Strong coupling constants. We use the Cartesian phase convention for baryon and meson states: $\pi^\pm$, $\Sigma^\pm \rightarrow (1 \pm i2)/\sqrt{2}$; π^0, $\Sigma^0 \rightarrow 3$; $K^\pm$, p, $\Xi^- \rightarrow (4 \pm i5)/\sqrt{2}$; K^0, $\bar{K}^0$, n, $\Xi^0 \rightarrow (6 \pm i7)/\sqrt{2}$; η_8, $\Lambda \rightarrow 8$ for $(d/f)_P \approx 1.74$, $(d+f)_P = 1$, $d_P \approx 0.635$, $f_P \approx 0.365$.

$g_{\pi^- pn}, g_{\pi^+ np}$	$= \sqrt{2}g$	$\simeq 19.0$
$g_{\pi^0 pp}, -g_{\pi^0 nn}$	$= g$	$\simeq 13.4$
$g_{\pi^-\Sigma^+\Lambda}, g_{\pi^0\Sigma^0\Lambda}, g_{\pi^-\Lambda\Sigma^-},$ $g_{\pi^+\Lambda\Sigma^+}, g_{\pi^0\Lambda\Sigma^0}$	$= \frac{2}{\sqrt{3}}d_P g$	$\simeq 9.8$
$g_{\pi^0\Sigma^+\Sigma^+}, g_{\pi^-\Sigma^0\Sigma^-}, -g_{\pi^+\Sigma^0\Sigma^+}$	$= 2f_P g$	$\simeq 9.8$
$g_{\pi^0\Xi^0\Xi^0}$	$= g(f-d)_P$	$\simeq -3.6$
$g_{\pi^-\Xi^0\Xi^-}$	$= \sqrt{2}g(d-f)_P$	$\simeq 5.1$

$$B(\Sigma_-^-) = \frac{g_{\pi^-\Sigma^0\Sigma^-}\langle n|H_w^{PC}|\Sigma^0\rangle}{m_\Sigma - m_n} + \frac{g_{\pi^-\Lambda\Sigma^-}\langle n|H_w^{PC}|\Lambda\rangle}{m_\Lambda - m_n} , \qquad (7b)$$

$$B(\Sigma_+^+) = \frac{g_{\pi^+\Sigma^0\Sigma^+}\langle n|H_w^{PC}|\Sigma^0\rangle}{m_\Sigma - m_n} + \frac{g_{\pi^+\Lambda\Sigma^+}\langle n|H_w^{PC}|\Lambda\rangle}{m_\Lambda - m_n}$$
$$- \frac{g_{\pi^+ np}\langle p|H_w^{PC}|\Sigma^+\rangle}{m_\Sigma - m_p} . \qquad (7c)$$

By inserting (4) and (6) into the above equations, and using the measured numbers for these B from Table I, the following self-consistent values for $\langle n|H_w^{PC}\Sigma^0\rangle$ are found:

$$\langle n|H_w^{PC}|\Sigma^0\rangle = \begin{cases} 130 \pm 8 \text{ eV} \quad (\Lambda_0^0) , \\ 123 \pm 5 \text{ eV} \quad (\Sigma_-^-) , \\ 124 \pm 20 \text{ eV} \quad (\Sigma_+^+) . \end{cases} \qquad (8a)$$

This consistency implies that indeed these B amplitudes are $\Delta I = \frac{1}{2}$ dominated with

$$\langle n|H_w^{PC}|\Sigma^0\rangle = -\langle p|H_w^{PC}|\Sigma^+\rangle/\sqrt{2} \approx 127 \text{ eV} . \qquad (8b)$$

Then the values (4), (6), and (8) for the three transitions are all compatible. Furthermore, the close agreement of the three pole model values of $\langle n|H_w^{PC}|\Sigma^0\rangle$ in (8a), with the expected $\Delta I = \frac{1}{2}$ value in (8b) (also found from the pole model), tells us that the pole model for p waves is extremely reliable.

The decays $\Xi^0 \rightarrow \Lambda\pi^0(\Xi_0^0)$ and $\Xi^- \rightarrow \Lambda\pi^-(\Xi_-^-)$ pose a more difficult problem since their pole graphs involve three reduced matrix elements $\langle \Lambda|H_w^{PC}|\Xi^0\rangle$, $\langle \Sigma^-|H_w^{PC}|\Xi^-\rangle$, and $\langle \Sigma^0|H_w^{PC}|\Xi^0\rangle$, but we can (again) use the $\Delta I = \frac{1}{2}$ rule to eliminate the latter transition via $\langle \Sigma^-|H_w^{PC}|\Xi^-\rangle = -\sqrt{2}\langle \Sigma^0|H_w^{PC}|\Xi^0\rangle$. This then gives two equations for two unknowns. However, this linear system has a determinant that is close to zero, making the uncertainties in the transitions so large that the values obtained are virtually useless. Another approach is to find an estimate for one of these reduced matrix elements and then solve for the other two transitions. As we will see later, the radiative decay $\Xi^- \rightarrow \Sigma^-\gamma$ will give a crude estimate for $\langle \Sigma^-|H_w^{PC}|\Xi^-\rangle$. Once we have this reduced matrix element we will then calculate $\langle \Lambda|H_w^{PC}|\Xi^0\rangle$ and $\langle \Sigma^0|H_w^{PC}|\Xi^0\rangle$.

III. OCTET RADIATIVE $B \rightarrow B'\gamma$ DECAYS

An independent way to test the scale of $\langle p|H_w|\Sigma^+\rangle$ is through the radiative decay $\Sigma^+ \rightarrow p\gamma$. If we again apply

octet-pole dominance as in Fig. 2, and define the amplitude as $M_\mu(B \to B'\gamma) = e(C + i\gamma_5 D\gamma_5 D)\sigma_{\mu\nu}k^\nu$, we can write the PC amplitude C as

$$C(\Sigma^+ \to p\gamma) = \frac{-\langle p|H_w^{PC}|\Sigma^+\rangle}{m_\Sigma - m_p}\left[\frac{\kappa_p}{2m_p} - \frac{\kappa_{\Sigma^+}}{2m_\Sigma}\right], \qquad (9)$$

where $\kappa_p, \kappa_{\Sigma^+}$ are anomalous magnetic moments. Although $\langle B'|H_w^{PV}|B\rangle = 0$, so that the D octet pole amplitude is zero here, decuplet intermediate states suggest[9] $D < 0$. The C amplitude can be determined from the decay rate and asymmetry parameter where

$$\Gamma(B \to B'\gamma) = \frac{e^2}{8\pi}\left[\frac{m_B^2 - m_{B'}^2}{m_B}\right]^3(C^2 + D^2), \qquad (10\text{a})$$

$$\alpha(B \to B'\gamma) = \frac{2CD}{C^2 + D^2}, \qquad (10\text{b})$$

we again take C and D real. The experimental values[2] $\Gamma(\Sigma^+ \to p\gamma) = (1.02 \pm 0.07) \times 10^{-17}$ GeV and $\alpha(\Sigma^+ \to p\gamma) = -0.83 \pm 0.12$ give, from (10),

$$C(\Sigma^+ \to p\gamma) = (1.55 \pm 0.13) \times 10^{-7}\ \text{GeV}^{-1}. \qquad (11)$$

Then by assuming the SU(3) values for the anomalous magnetic moments $\kappa_{\Sigma^+} = \kappa_p \approx 1.79$, we obtain from (9) and (11),

$$\langle p|H_w^{PC}|\Sigma^+\rangle = -193 \pm 16\ \text{eV}. \qquad (12)$$

This agrees quite well with the value obtained in (4) for $\Sigma^+ \to p\pi^0$ decay and suggests again that the pole model is very reliable for PC p waves.

The next radiative decay of interest is $\Xi^- \to \Sigma^-\gamma$. The graphs analogous to Fig. 2 and (9) now give

$$C(\Xi^- \to \Sigma^-\gamma) = \frac{-\langle \Sigma^-|H_w^{PC}|\Xi^-\rangle}{m_\Xi - m_\Sigma}\left[\frac{\kappa_{\Sigma^-}}{2m_\Sigma} - \frac{\kappa_{\Xi^-}}{2m_\Xi}\right]. \qquad (13)$$

The experimental[2] decay rate is $\Gamma(\Xi^- \to \Sigma^-\gamma) = (9.2 \pm 4.0) \times 10^{-19}$ GeV, with no measured value for the asymmetry parameter. However, the latter can be circumvented since in the SU(3) limit there are no decuplet pole contributions, suggesting $D(\Xi^- \to \Sigma^-\gamma) = 0$. Therefore from (10a) we find

$$C(\Xi^- \to \Sigma^-\gamma) = (1.4 \pm 0.3) \times 10^{-7}\ \text{GeV}^{-1}. \qquad (14)$$

Using the experimentally determined values for the anomalous magnetic moments $\kappa_{\Xi^-} \approx 0.03$ and $\kappa_{\Sigma^-} \approx 0.48$ in Eq. (13), it follows that
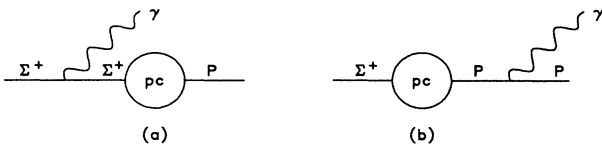
$$|\langle \Sigma^-|H_w^{PC}|\Xi^-\rangle| = 80 \pm 20\ \text{eV}. \qquad (15)$$

As promised in the preceding section, once $\langle \Sigma^-|H_w^{PC}|\Xi^-\rangle$ was known we could find the reduced matrix elements $\langle \Lambda|H_w^{PC}|\Xi^0\rangle$ and $\langle \Sigma^0|H_w^{PC}|\Xi^0\rangle$. The pole graphs analogous to Fig. 1 lead to the following equations for $B(\Xi \to \Lambda\pi)$:

$$B(\Xi_-^-) = \frac{g_{\pi^-\Xi^0\Xi^-}\langle \Lambda|H_w^{PC}|\Xi^0\rangle}{m_\Xi - m_\Lambda}$$

$$- \frac{g_{\pi^-\Lambda\Sigma^-}\langle \Sigma^-|H_w^{PC}|\Xi^-\rangle}{m_\Xi - m_\Sigma}, \qquad (16\text{a})$$

$$B(\Xi_0^0) = \frac{g_{\pi^0\Xi^0\Xi^0}\langle \Lambda|H_w^{PC}|\Xi^0\rangle}{m_\Xi - m_\Lambda} - \frac{g_{\pi^0\Lambda\Sigma^0}\langle \Sigma^0|H_w^{PC}|\Xi^0\rangle}{m_\Xi - m_\Sigma}. \qquad (16\text{b})$$

Using the values of B from Table I, the couplings from Table II, and the magnitude for $\langle \Sigma^-|H_w|\Xi^-\rangle$ found in (15), then Eqs. (16) give

$$\langle \Lambda|H_w^{PC}|\Xi^0\rangle = -180 \pm 60\ \text{eV}, \qquad (17\text{a})$$

$$\langle \Sigma^0|H_w^{PC}|\Xi^0\rangle = 55 \pm 15\ \text{eV}. \qquad (17\text{b})$$

The magnitude and sign of the above transitions come from assuming $\langle \Sigma^-|H_w|\Xi^-\rangle < 0$. As can be seen from (15) and (17b), $\langle \Sigma^-|H_w|\Xi^-\rangle \approx -\sqrt{2}\langle \Sigma^0|H_w|\Xi^0\rangle$ as required by SU(2) and the $\Delta I = \frac{1}{2}$ rule.

IV. W-EXCHANGE QUARK MODEL

It was first appreciated in Refs. 3 and 10 that the W-exchange quark model for qqq baryons when combined with the color symmetry of the three quarks in fact generates a $\Delta I = \frac{1}{2}$ weak Hamiltonian density H_{Wx}. As a first estimate of this W-exchange quark graph of Fig. 3 for the $\langle B'|H_w^{PC}|B\rangle$ transitions, we follow the nonrelativistic W-exchange approach of Riazuddin and Fayyazuddin.[5] Then the parity-conserving Hamiltonian density has the form

$$H_{Wx}^{PC} = (G_F/\sqrt{2})s_1c_1\sum_{i > j}(\alpha_i^-\beta_j^+ + \beta_i^+\alpha_j^-)(1 - \sigma_i \cdot \sigma_j)\delta^3(\mathbf{r}), \qquad (18)$$

where α_i^- and β_j^+ transform a u into a d quark and as s into a u quark, respectively. This gives, for example

$$\langle p|H_{Wx}^{PC}|\Sigma^+\rangle = (G_F/\sqrt{2})(-6)s_1c_1\langle \psi_0|\delta^3(\mathbf{r})|\psi_0\rangle$$

$$\approx -90\ \text{eV} \qquad (19)$$

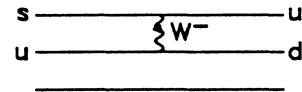for $s_1c_1 \approx 0.221$. Here the factor of (-6) comes from us-

FIG. 2. Octet-pole graphs for $\Sigma^+ \to p\gamma$ decay.

FIG. 3. W-exchange quark graph for qqq baryons.

TABLE III. Pole-model vs W-exchange plus self-energy PC transitions.

	Expt. (eV)	W-x (eV)	Self-energy (eV)	W-x + SE (eV)
$\langle p|H_w^{PC}|\Sigma^+\rangle$	-180 ± 10	-90	-60	-150
$\langle n|H_w^{PC}|\Sigma^0\rangle$	125 ± 10	65	40	105
$\langle n|H_w^{PC}|\Lambda\rangle$	-87 ± 4	-35	-70	-105
$\langle \Sigma^-|H_w^{PC}|\Xi^-\rangle$	-80 ± 20	0	-70	-70
$\langle \Sigma^0|H_w^{PC}|\Xi^0\rangle$	55 ± 15	0	50	50
$\langle \Lambda|H_w^{PC}|\Xi^0\rangle$	-180 ± 60	-70	-80	-150

ing SU(6) wave functions for the qqq baryons[11] and the contact matrix element in (19) is estimated from the strong-interaction Δ-N mass splitting to be[12]

$$\langle \psi_0|\delta^3(\mathbf{r})|\psi_0\rangle \approx \frac{3(\Delta - N)}{8\pi\alpha_s}m_u^2 \approx 8\times10^{-3} \text{ GeV}^3 \qquad (20)$$

for $\alpha_s(1 \text{ GeV})\approx0.5$ and $m_u\approx0.34$ GeV.

The other $\langle B'|H_{Wx}^{PC}|B\rangle$ values are listed in Table III. The form of the equations for these transitions is the same as Eq. (19) save for the Clebsch-Gordan coefficients. The latter are[5] -6, $-\sqrt{6}$, $3\sqrt{2}$, $-2\sqrt{6}$ for the W-exchange graphs of $\langle p|H_{Wx}^{PC}|\Sigma^+\rangle$, $\langle n|H_{Wx}^{PC}|\Lambda\rangle$, $\langle n|H_{Wx}^{PC}|\Sigma^0\rangle$, and $\langle \Lambda|H_{Wx}^{PC}|\Xi^0\rangle$, respectively. In Table III the ratio $\langle p|H_{Wx}^{PC}|\Sigma^+\rangle/\langle n|H_{Wx}^{PC}|\Sigma^0\rangle$ is numerically close to $-\sqrt{2}$ as expected from SU(2) symmetry and the $\Delta I=\frac{1}{2}$ rule. However, the transitions $\langle \Sigma|H_w^{PC}|\Xi\rangle$ cannot have a W exchanged between an ssd or ssu Ξ baryon and an sdd or suu Σ baryon; hence,

$$\langle \Sigma|H_{Wx}|\Xi\rangle = 0 . \qquad (21)$$

Table III clearly shows that the W-exchange model is lacking; not only are the nonvanishing W-exchange transitions about *one-half* the pole-model empirical values, but $\langle \Sigma|H_w^{PC}|\Xi\rangle$ is definitely *not* zero in contrast with the vanishing W-exchange transition (21).

V. DECUPLET BARYON $D \to B\pi$ DECAYS

As we have seen in the preceding section, the W-exchange quark model does not predict accurately the observed $\langle B'|H_w^{PC}|B\rangle$ transitions. In particular there are no W-exchange graphs for the two $\langle \Sigma|H_w^{PC}|\Xi\rangle$ transitions, which are clearly nonzero. Similarly, there is no W-exchange graph for the decuplet-baryon transition $\langle \Xi|H_w^{PV}|\Omega\rangle$, which as we will show in this section is empirically nonzero. This gives added incentive to find a quark supplement to the W-exchange quark model, which we will present in the next section. First we will demonstrate that $\langle \Xi|H_w^{PV}|\Omega\rangle$ is nonzero and obtain an approximate phenomenological value for this PV reduced matrix element.

We extract the dominant $\Delta I=\frac{1}{2}$ component of H_w from $\Omega\to\Xi\pi$ weak decays with PC and PV amplitudes defined by

$$\langle \pi\Xi|H_w|\Omega\rangle = -\bar{u}(\Xi)(E_{PC}+i\gamma_5 F_{PV})p_\mu^B u^\mu(\Omega) ,$$

where $u^\mu(\Omega)$ is the Rarita-Schwinger spin-$\frac{3}{2}$ bispinor satisfying $p^\Omega u(\Omega)=0$ and our choice of metric and γ matrices agrees with Ref. 1. The decay rate for $\Omega\to\Xi\pi$ is

dominated by the PC amplitude

$$\Gamma = \frac{p^3}{12\pi m_\Omega}[(E_\Xi+m_\Xi)|E_{PC}|^2+(E_\Xi-m_\Xi)|F_{PV}|^2]$$

$$\approx \frac{p^3}{24\pi m_\Omega^2}(m_\Omega+m_\Xi)^2|E_{PC}|^2 . \qquad (22)$$

The kinematic dominance of E_{PC} over F_{PV} will simplify the analysis considerably, and henceforth we shall neglect the small PV amplitude F_{PV}. Accordingly we write the reduced $\Omega^-\to\Xi^-$ weak PV transition as

$$\langle \Xi^-|H_w^{PV}|\Omega^-\rangle = -ih_2\bar{u}(\Xi)p_\mu^B u^\mu(\Omega) . \qquad (23)$$

Since the isospin of Ω is zero, the amplitude h_2 is a pure $\Delta I=\frac{1}{2}$ weak transition.

To proceed we invoke the usual chiral (left-handed) current algebra $[Q_5,H_w^{PC}]=-[Q,H_w^{PV}]$. Applying the latter and PCAC to evaluate $\Omega^-\to\Xi^-\pi^0$ decay one finds[9]

$$\langle \pi^0\Xi^-|H_w^{PC}|\Omega^-\rangle \approx (i/f_\pi)\langle \Xi^-|[Q^3,H_w^{PV}]|\Omega^-\rangle$$

$$= -(i/2f_\pi)\langle \Xi^-|H_w^{PV}|\Omega^-\rangle , \qquad (24a)$$

$$E_{PC}(\Xi^-\pi^0)\approx h_2/2f_\pi . \qquad (24b)$$

Likewise for $\Omega^-\to\Xi^0\pi^-$ decay this current-algebra–PCAC procedure gives $E_{PC}(\Xi^0\pi^-)\approx -h_2/\sqrt{2}f_\pi$. For $f_\pi\approx93$ MeV, the observed branch ratios[2] 8.6% and 23.6% along with lifetime $\tau_\Omega\approx0.822\times10^{-10}$ sec, respectively, give the amplitudes from (22), $|E(\Xi^-\pi^0)|\approx0.80\times10^{-6}$ GeV^{-1} and $|E(\Xi^0\pi^-)|\approx1.33\times10^{-6}$ GeV^{-1}. Then the $\Delta I=\frac{1}{2}$ weak transition, respectively, has dimensionless magnitude

$$|h_2|\approx0.15\times10^{-6}, \quad 0.18\times10^{-6} . \qquad (25)$$

The discrepancy between these two values for h_2 is the measure of the small $\Delta I=\frac{3}{2}$ component in $\Omega\to\Xi\pi$.

An independent way to determine this $\Delta I=\frac{1}{2}$ weak transition h_2 is to begin with $\langle \Xi^-|H_w^{PV}|\Omega^-\rangle$ and (kaon) pole dominating it as depicted by the kaon tadpole graph of Fig. 4. This corresponds to the tadpole transition

$$\langle \Xi^-|H_w^{PV}|\Omega^-\rangle = \langle 0|H_w^{PV}|\overline{K}^0\rangle m_K^{-2}g_{\Omega K\Xi}\bar{u}(\Xi)p_\mu^B u^\mu(\Omega) , \qquad (26)$$

where $g_{\Omega K\Xi}=\sqrt{2}/f_K\approx12$ GeV^{-1} is the Goldberger-Treiman relation for spin $\frac{3}{2}^+\to\frac{1}{2}^+$ transitions (consistent with $g_{\pi\Delta N}$). Also current algebra and PCAC link
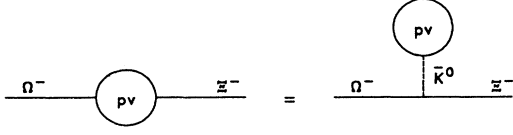
FIG. 4. Hadronic kaon PV tadpole dominance of $\langle \Xi^- | H_w^{PV} | \Omega^- \rangle$.

$\bar{K}^0 \to 2\pi$ to $\bar{K}^0 \to 0$ as[1]

$$\langle \pi\pi | H_w^{PV} | \bar{K}^0 \rangle \approx (-1/2f_\pi^2)\langle 0 | H_w^{PV} | \bar{K}^0 \rangle (1 - m_\pi^2/m_K^2) \ .$$

$$(27)$$

Using the measured[2] $\bar{K}_{2\pi}^0$ decay rate requires $|\langle \pi\pi | H_w^{PV} | \bar{K}^0 \rangle| \approx 26 \times 10^{-8}$ GeV or $|\langle 0 | H_w^{PV} | \bar{K}^0 \rangle| \approx 4.9 \times 10^{-9}$ GeV^3. Then (23), (26), and (27) predict

$$|h_2| \approx |\langle 0 | H_w^{PV} | \bar{K}^0 \rangle m_K^{-2} g_{\Omega K \Xi}| \approx 0.24 \times 10^{-6} \ , \quad (28)$$

reasonably close to the phenomenological values (25) found from $\Omega \to \Xi\pi$ decays.

Also h_2 can be found from s-wave PV $B \to B'\pi$ decay amplitudes A, which are listed in Table I. If we assume that only the current algebra contributes to s waves, then, e.g., the PV $\Sigma^+ \to p\pi^0$ amplitude is predicted to be

$$A(\Sigma_0^+) = i\langle \pi^0 p | H_w^{PV} | \Sigma^+ \rangle = (1/2f_\pi)\langle p | H_w^{PC} | \Sigma^+ \rangle$$

$$\approx -0.97 \times 10^{-6} \ , \quad (29)$$

where we have used $\langle p | H_w^{PC} | \Sigma^+ \rangle \approx -180$ eV from our pole model fits (4) and (12). We note that (29) is over twice the observed $A(\Sigma_0^+)$ amplitude in Table I. To explain this long-appreciated s-wave mismatch, one should add PV decuplet pole contributions that in fact are proportional to h_2. Then the above s-wave mismatch is resolved if h_2 assumes the value[1,9]

$$h_2 \approx -0.2 \times 10^{-6} \ , \quad (30)$$

again compatible with (25) and (28).

VI. QUARK TADPOLE MODEL FOR $\Omega \to \Xi\pi$ DECAYS

First we note that there can be no W exchanged between sss and ssd or ssu hadrons, so that $\langle \Xi | H_{Wx} | \Omega \rangle = 0$, inconsistent with the nonvanishing h_2 in the preceding section. This null result is analogous to $\langle \Sigma | H_{Wx} | \Xi \rangle = 0$ from (21) and convinces us that there *must* be another $\Delta I = \frac{1}{2}$ quark graph mechanism in addition to W exchanges, because $\langle \Xi | H_w^{PV} | \Omega \rangle$ and $\langle \Sigma | H_w^{PC} | \Xi \rangle$ certainly exist. Second we recall from Fig. 4 and (28) that a tadpole description of $\langle \Xi | H_w^{PV} | \Omega \rangle$ exists with a $\bar{K}^0$ pole [linked to the observed $K_{2\pi}^0$ decays via the current-algebra–PCAC relation (27)] generating a PV scale h_2 compatible with $\Omega \to \Xi\pi$ data in Sec. V.

The above two clues naturally suggest that a tadpole-like $\Delta I = \frac{1}{2}$, $\Delta S = 1$ PV component of H_w should also exist at the quark level, which we denote as H_{tad}^{PV}. Expressing this PV and PC Hermitian H_w as $H_{tad} = \Sigma_{sd} + \Sigma_{ds}$, the quark tadpole s-d self-energy graph Σ_{sd} is shown in Fig. 5(a). It is most convenient to evaluate Σ_{sd} in the 't
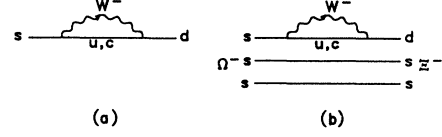

FIG. 5. Quark s-d tadpole self-energy (a), and contribution to $\langle \Xi^- | H_{tad}^{PV} | \Omega^- \rangle$ in (b).

Hooft–Feynman gauge $g_{\mu\nu}$ for the W propagator, because then the *left-handed* (LH) structure of the W-quark vertices translates to a LH structure for the self-energy Σ_{sd}, since $g^{\mu\nu}\gamma_\mu^{LH}(\not{p} + m)\gamma_\nu^{LH} = -4\not{p}^{LH}$. Only then does the usual LH current-algebra $[Q_5 + Q, H_w^{LH}] = 0$ structure of the quark current[13] become manifest. In Feynman gauge the Glashow-Iliopoulos-Maiani SU(4) structure of the quark current requires Σ_{sd} to take the low-momentum form[1]

$$\Sigma_{sd} = b(p^2)\bar{d}\not{p}(1 - i\gamma_5)s,$$

$$(31)$$

$$b(p^2 \approx 0) = b \approx -\frac{G_F}{8\pi^2\sqrt{2}}s_1 c_1(m_c^2 - m_u^2) \approx -5.6 \times 10^{-8}$$

for $s_1 c_1 \approx 0.221$, $m_c \approx 1.6$ GeV, $m_u \approx 0.34$ GeV. Away from Feynman gauge $a = 1$, Eq. (31) remains approximately valid in other (non-Landau) covariant gauges with small corrections proportional to $(a - 1)(m_s - m_d)^2/M_W^2$, due to additional unphysical-Higgs-boson χ^- contributions.[14]

In spite of our knowledge of (31) as early[15] as 1979, some physicists have discarded (31) on the grounds that it can be "transformed or diagonalized" away. While a direct s-d transition can be removed through semistrong or e^2 electroweak order, Weinberg[16] demonstrated that a "truly weak" interaction (such as Σ_{sd}) *cannot* be removed through $O(e^2 m_c^2/M_W^2)$, which is the scale of (31). Another way to see that the transforming away issue has been implicitly accounted for above is to express the overall d and s self-energy operators in matrix form

$$A = \begin{bmatrix} \Sigma_{dd} & \Sigma_{sd} \\ \Sigma_{sd} & \Sigma_{ss} \end{bmatrix} ,$$

with quark and hadron flavor diagonalized only through strong and semistrong order, where $\Sigma_{sd} \neq 0$, $\langle \pi | H_w | K \rangle \neq 0$. If one instead diagonalizes flavor through strong and weak interactions, then the self-energy matrix can be transformed to

$$B = \begin{bmatrix} \tilde{\Sigma}_{dd} & 0 \\ 0 & \tilde{\Sigma}_{ss} \end{bmatrix} ,$$

with the transformation (mixing) angle ϕ satisfying $\frac{1}{2}\sin 2\phi = \Sigma_{sd}(\tilde{\Sigma}_{ss} - \tilde{\Sigma}_{dd})^{-1}$ and $\tilde{\Sigma}_{ss}, \tilde{\Sigma}_{dd}$ corresponding to constituent quark masses $m_{s,d}$. Thus, either one works with (31) and the matrix A with $\Sigma_{sd} \neq 0$ or instead transforms away $\tilde{\Sigma}_{sd} = 0$ in B. In the latter case Σ_{sd} is recovered via the small mixing angle $\phi \sim 10^{-6}$, which is now buried into the new definition of flavor states.

Returning to (31), the $K_{2\pi}^0$ matrix elements are[17]

$$i\langle \pi\pi|H_w^{PV}|\bar{K}^0\rangle \approx (f_K/f_\pi^2)\sqrt{2}b(m_K^2-m_\pi^2)$$

$$\approx -24\times 10^{-8} \text{ GeV} , \tag{32a}$$

$$-i\langle 0|H_w^{PV}|\bar{K}^0\rangle \approx 2\sqrt{2}bf_Km_K^2 , \tag{32b}$$

consistent with the current-algebra–PCAC relation (27) and compatible with $K_{2\pi}^0$ data. In the Appendix we shall derive (32) from the tadpole form of H_w in (31). Here we apply this s-d $\Delta I=\frac{1}{2}$ weak tadpole to the $\Omega^-\to\Xi^-$ transition of Fig. 5(b), giving[18]

$$\langle \Xi^-|\Sigma_{sd}|\Omega^-\rangle = -ih_2\bar{u}(\Xi)p_\mu^\Xi u^\mu(\Omega) . \tag{33}$$

Then the Goldberger-Treiman-type identity $g_{\Omega K^0\Xi}=\sqrt{2}/f_K$ combined with the tadpole relations (28) and (32) predict

$$h_2=2\sqrt{2}bf_Km_K^2m_K^{-2}\sqrt{2}/f_K=4b\approx -0.22\times 10^{-6} . \tag{34}$$

We believe it is significant that this quark-tadpole prediction is compatible with the previous estimates of h_2 in (25), (28) and (30).

VII. QUARK SELF-ENERGY COMPONENT OF $B\to B'\pi$ DECAYS

We showed in the previous section that the quark self-energy Σ_{sd} produces a nonzero PV weak transition $\langle \Xi|\Sigma_{sd}^{PV}|\Omega\rangle$ which is close to experiment. Here we will apply the same procedure to the hyperon PC transitions $\langle B'|\Sigma_{sd}^{PC}|B\rangle$, where the latter will supplement the four nonzero W-exchange elements and also the two transitions (21) that are predicted zero by W exchange. In contrast with the preceding section, while the Ω tadpole decays requires the PV part of the self-energy Hamiltonian (31), the PC hyperon $B\to B'$ transition will use the PC part $\Sigma_{sd}^{PC}=bd\bar{p}s$. Such a PC self-energy component of H_w, although being of the Σ_{sd}^{PC} form, is *not* a tadpole for $B\to B'\pi$ decays [the analog κ tadpole graph similar to Fig. 4 for $\langle B'|H_w^{PC}|B\rangle$ transitions is SU(3) suppressed]. Furthermore one knows[19] that possible PC baryon tadpole graphs would vanish (if H_{Wx} were zero). However, we can express the qqq baryon matrix elements of Σ_{sd}^{PC} in the following factorized non-SU(3)-suppressed form:

$$\langle B^f|\Sigma_{sd}^{PC}|B^i\rangle = -(if^{f6i})b(m_f+m_i) , \tag{35}$$

where from (31) Σ_{sd} converts an s to a d quark with weak scale b and transforms as the SU(3) $\Delta I=\frac{1}{2}$ operator λ_6. Covariant normalization $(\bar{u}u=2m)$ suggests the factor (m_f+m_i) in (35). The Clebsch-Gordan coefficient f^{f6i} in (35) is Gell-Mann's SU(3)-antisymmetric structure constant. In quark-spectator language this f-type coupling follows from the SU(3) characteristics of a single quark line.

Applying (35) to the six transitions of interest yields

$$\langle p|\Sigma_{sd}^{PC}|\Sigma^+\rangle = (b/2)(m_\Sigma+m_N)\approx -60 \text{ eV} , \tag{36a}$$

$$\langle n|\Sigma_{sd}^{PC}|\Sigma^0\rangle = -(b/2\sqrt{2})(m_\Sigma+m_N)\approx 40 \text{ eV} , \tag{36b}$$

$$\langle n|\Sigma_{sd}^{PC}|\Lambda\rangle = (\sqrt{3}b/2\sqrt{2})(m_\Lambda+m_N)\approx -70 \text{ eV} , \tag{36c}$$

$$\langle \Sigma^-|\Sigma_{sd}^{PC}|\Xi^-\rangle = (b/2)(m_\Xi+m_\Sigma)\approx -70 \text{ eV} , \tag{36d}$$

$$\langle \Sigma^0|\Sigma_{sd}^{PC}|\Xi^0\rangle = -(b/2\sqrt{2})(m_\Xi+m_\Sigma)\approx 50 \text{ eV} , \tag{36e}$$

$$\langle \Lambda|\Sigma_{sd}^{PC}|\Xi^0\rangle = (\sqrt{3}b/2\sqrt{2})(m_\Xi+m_\Lambda)\approx -80 \text{ eV} , \tag{36f}$$

where we have used $b\approx -56\times 10^{-9}$ as found in (31). There is an additional sign in the Ξ transitions due to the SU(6) qqq form of the Thirring wave functions.[11] The self-energy amplitudes (36) are a clear improvement when added to the W-exchange predictions of Table III. Of primary importance are the $\langle \Sigma|H_w^{PC}|\Xi\rangle$ matrix elements, which the W-exchange quark model predicted to be zero and are now close to the experiment.

VIII. CONCLUSION

First we gave a systematic procedure for extracting $\langle B'|H_w^{PC}|B\rangle$ from the $B\to B'\pi$, $B\to B'\gamma$ pole models as listed in Table III. The W-exchange quark-model Hamiltonian density H_{Wx}^{PC} generated reduced PC matrix elements in Table III, which only partly explained the data. Next we turned to decuplet $\Omega\to\Xi\pi$ PC transitions that after using current-algebra and PCAC techniques resulted in a PV scale $h_2\approx -0.2\times 10^6$, which could not be explained by H_{Wx}^{PV} since the latter vanishes. However, the observed h_2 could be understood from the tadpole Σ_{sd}^{PV} realization of H_w^{PV} as $h_2=4b$. The PC (chiral) component of Σ_{sd}^{PC} also supplied the needed matrix elements of $\langle B'|H_w^{PC}|B\rangle$ in Table III.

Thus we deduce that the complete quark model form of the $\Delta I=\frac{1}{2}$ weak Hamiltonian density

$$H_w=H_{Wx}+\Sigma_{sd} \tag{37}$$

can predict all the experimental data for hyperon $B\to B'\pi$, $B\to B'\gamma$, and decuplet $\Omega\to\Xi\pi$ weak nonleptonic $\Delta I=\frac{1}{2}$ decays. The two W-exchange and self-energy Hamiltonians in (37) in effect resolve the s-wave $B\to B'\pi$ mismatch problem of (29), because then the H_{Wx} and Σ_{sd} contributions *subtract* in s wave [due to the minus sign in (31)]. Furthermore, the p-wave $B\to B'\pi$ problem stated after (21) is also resolved, because then the H_{Wx} and Σ_{sd} contributions *add* in p wave.

The striking consistency of our overall weak first-order perturbation-theory (FOPT) PC pole models in Secs. II and III and the PV tadpole picture in Sec. V means that the resulting six $\langle B'|H_w^{PC}|B\rangle$ transitions in Table III and $\langle B|H_w^{PV}|D\rangle\sim h_2$ are real physical quantities which cannot be "transformed away." Although FOPT has never been directly questioned for baryon decays, recently analog FOPT extractions for meson decays, i.e., $\langle \pi|H_w^{PC}|K\rangle$ and $\langle 0|H_w^{PV}|K\rangle$, have been dismissed and "transformed away." But the latter dismissal is not valid in FOPT because the K,π and vacuum states must then be taken as eigenstates of the strong and semistrong Hamiltonian H_s with the weak H_w sandwiched between these strong eigenstates. This FOPT picture is compatible with our tadpole approach to $\langle 0|H_w^{PV}|K\rangle$ in Sec. VI and in the Appendix, which is nonzero and cannot be transformed away in "old-fashioned" perturbation theory.

ACKNOWLEDGMENTS

APPENDIX

To convert the $\Delta I = \frac{1}{2}$ quark tadpole form of H_w in (31) to hadron transitions, we start with the Lehmann-Symanzik-Zimmermann form of the weak axial-vector amplitude

$$M_\mu = -i \int d^4x \, e^{iq \cdot x} \langle 0 | T(A_\mu^3(x) H_w) | \overline{K}^0 \rangle \ . \qquad (A1)$$

Then the divergence of (A1) integrated by parts in the soft limit combined with the usual LH charge algebra $[Q^3 + Q_5^3, H_w] = 0$ leads to the low-energy theorem

$$q^\mu M_\mu \to \langle 0 | [Q_5^3, H_w] | \overline{K}^0 \rangle = - \langle 0 | [Q^3, H_w] | \overline{K}^0 \rangle$$

$$= \tfrac{1}{2} \langle 0 | H_{\text{tad}} | \overline{K}^0 \rangle \ . \qquad (A2)$$

Here we assume $H_w = H_{Wx} + \Sigma_{sd}$, but only the tadpole part of H_w can contribute to the last vacuum (tadpole) $\overline{K}^0$ transition in (A2).

However, by analogy with the strong axial-vector s-d transition of Fig. 6(a),
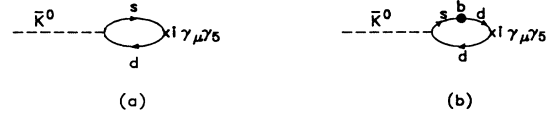

FIG. 6. Quark representation of the strong $\Delta S = 1$ axial-vector current (a), and of the weak $\Delta S = 1$ axial-vector current (b).

$$\langle 0 | A_\mu^{6+i7} | \overline{K}^0 \rangle = i f_K q_\mu \sqrt{2} \ , \qquad (A3)$$

we can approximate the weak axial-vector s-d tadpole transition of Fig. 6(b) (treated as an s-d "dot") as

$$M_\mu \approx b (i f_K q_\mu \sqrt{2}) \ . \qquad (A4)$$

Then computing $q^\mu M_\mu$ on the kaon mass shell $q^2 = m_K^2$ and comparing with (A2) we find

$$\langle 0 | \Sigma_{sd}^{\text{PV}} | \overline{K}^0 \rangle \approx 2\sqrt{2} b i f_K m_K^2 \ , \qquad (A5)$$

which is as stated in (32b). The factor of $\frac{1}{2}$ in the current-algebra–PCAC relation (27) converting (32b) to (32a) is due to a (rapidly varying) kaon tadpole.[1]

[1]See, e.g., M. D. Scadron, Rep. Prog. Phys. **44**, 213 (1981), and references therein.

[2]Particle Data Group, G. P. Yost *et al.*, Phys. Lett. B **204**, 1 (1988).

[3]J. C. Pati and C. H. Woo, Phys. Rev. D **3**, 2920 (1971).

[4]C. Schmid, Phys. Lett. **66B**, 353 (1977).

[5]Riazuddin and Fayyazuddin, Phys. Rev. D **18**, 1478 (1978); **19**, 1630(E) (1978).

[6]Our choice of relative signs for the A and B in Table I derives from a Cartesian phase convention for baryon states (see Table II and Ref. 1).

[7]L. S. Brown and C. M. Sommerfield, Phys. Rev. Lett. **16**, 761 (1966).

[8]Most recent estimates for the axial-vector-current ratio $(d/f)_A \approx 1.74$ are in Z. Dziembowski and J. Franklin, Temple University Report No. TUHE-89-11, 1989 (unpublished); F. E. Close, Phys. Rev. Lett. **64**, 361 (1990); M. Roos, in Proceedings of the 25th International High Energy Physics Conference, Singapore, 1990 (to be published).

[9]M. D. Scadron and L. R. Thebaud, Phys. Rev. D **8**, 2190 (1973); M. D. Scadron and M. Visinescu, *ibid.* **28**, 1117 (1983).

[10]Also see J. G. Körner, Nucl. Phys. **B25**, 282 (1970).

[11]W. Thirring, Acta Phys. Austriaca Suppl. **II**, 205 (1966); J. Kokkedee, *The Quark Model* (Benjamin, New York, 1969), p. 187.

[12]A. DeRújula, H. Georgi, and S. Glashow, Phys. Rev. D **12**, 147 (1975).

[13]S. Glashow, J. Iliopoulos, and L. Maiani, Phys. Rev. D **2**, 1285 (1970).

[14]See, e.g., V. Elias, D. G. C. McKeon, and M. D. Scadron, Can. J. Phys. (to be published).

[15]P. Pascual and R. Tarrach, Phys. Rev. Lett. **87B**, 64 (1979); M. D. Scadron, *ibid.* **95B**, 123 (1980).

[16]S. Weinberg, Phys. Rev. D **8**, 605 (1973); Phys. Rev. Lett. **31**, 494 (1973).

[17]N. H. Fuchs and M. D. Scadron, Nuovo Cimento A **93**, 205 (1986); R. Delbourgo and M. D. Scadron, Nuovo Cimento Lett. **44**, 193 (1985).

[18]M. P. Khanna, R. C. Verma, and M. D. Scadron, J. Phys. G **12**, B23 (1986).

[19]S. Coleman and S. Glashow, Phys. Rev. **134**, B671 (1964).